

Study on behaviour of corroded RC beams repaired in shear with NSM CFRP rods

Belal ALMASSRI¹, Amjad KREIT¹, Firas AL MAHMOUD², Raoul FRANCOIS¹

¹University of Toulouse; UPS, INSA, LMDC (Laboratoire Matériaux et Durabilités des Constructions), France

²Institut Jean Lamour, CP2S, Nancy Université UPVM, CNRS, IUT NB, 54601 Villers-lès-Nancy, France

Abstract. The near surface mounted reinforcement technique (NSM) is one of the promising techniques used nowadays. In the NSM technique, the Carbon Fibre Reinforced Polymer (CFRP) rods are placed inside pre-cut grooves and are bonded to the concrete with epoxy adhesive. Experimental results obtained on concrete short beams taken from one beam exposed to a natural corrosion for 25 years then repaired only in flexion or in flexion and shear are reported. Results were compared to control beams. One 6-mm-diameter NSM CFRP rod is used to repair the beams. The beams were tested statically in three-point bending up to failure. Results showed that the failure mode of all repaired RC beams in flexion was by shear failure after CFRP rods slip. But the failure mode of the corroded RC beams repaired in both flexion and shear occurred due to concrete crushing. An increase was noticed in the ultimate shear capacity of those repaired beams.

1 Introduction

The cost increase due to the rehabilitation of the deteriorated RC structures reaches to millions of euros each year. The corrosion of the steel bars in the RC elements leads to a reduction in the cross sectional area of the steel reinforcement and a significant reduction in its ductility which leads to the early failure of steel bars, [1, 2]. The near surface mounted reinforcement technique (NSM) is one of the promising techniques used nowadays. In the NSM technique, the Carbon Fibre Reinforced Polymer (CFRP) rods are placed inside pre-cut grooves and are bonded to the concrete with epoxy adhesive. [3] presented a testing program in order to assess the increasing of the shear capacity can happen by using the NSM FRP reinforcement technique, this test program tested the beams in two regions. The increase of the shear capacity was between 22% - 44% for beams strengthened with NSM reinforcement,

Another research done by [4] used the Manually Made FRP rods (MMFRP), the strong shear region was reinforced with $\varnothing 8$ every 50mm and the weak one was $\varnothing 6$ every 150mm, in order to ensure high degree of anchorage the MMFRP rods were fixed at an incline angle 45 degrees to the beam axis and it was covered with more dry fibre at the ends with wooden core to wrap the fibres around it, the failure mode was a diagonal cracking in the beam followed by splitting large parts of the concrete cover and the increase in the shear capacity was between 25% - 48%. [5] suggested some of recommended methods that can increase the shear capacity of the strengthened T-beams by decreasing the spacing between the FRP rods and by increasing the length of anchorage of the FRP rods in the T-beam to be anchored also into the flange and finally it recommended sort of inclination degrees by 45 degrees in the FRP rods

rather than to be vertical as this will increase the shear capacity of the reinforced concrete elements.

[6] reported the test results of a single full-scale PC girder taken from a bridge and shear-strengthened with NSM CFRP strips. The beam failed in flexure at a shear force close to the shear resistance predicted by the model given in [7] this model which presented some results prove that the use of NSM FRP rods improves the shear capacity of reinforced concrete beams where in absence of steel stirrups (shear reinforcement), an increase happened in the shear capacity comes to 105.7% with respect to the control beam while the strengthened beam showed an increase in the shear capacity of 35% over the unstrengthened one. The failure mode found by this research to be splitting the FRP rods due to splitting the epoxy cover. The aim of our paper is to investigate the post-repair performance of corrosion-damaged RC beams. Beams are repaired in flexion and shear with NSM CFRP rod. The beams were tested statically in three-point bending up to failure.

2 Experimental context

An experimental program was started at LMDC in 1984 aimed to understand the effects of the steel corrosion on the structural behavior of the RC elements. Many experimental studies were conducted on those beams to evaluate the development of corrosion cracking, to measure chloride content and to analyze the change of the mechanical behavior [8, 9]. The natural aggressive environment system is presented in [10].

The beams studied in this paper are one corroded beam (called A1CL3) and one control beam (called A1T). A1CL3 beam was loaded in three-point flexure to $M_{ser}=14$ kN.m. The control beam A1T was strengthened

using the same method as the one used to repair the corroded beam A1CL3. The layout of the reinforcement is shown in Figure. 1. For these beams, M_{ser} represented the maximum loading value versus the durability in an aggressive environment (serviceability limit-state requirements in an aggressive environment) and to maximum loading value versus resistance (ultimate load limit state in a non-aggressive environment) for the type B beam. M_{ser} represented 50% of the failure load, and the maximum stress in the tensile steels σ_s which was 240 MPa. Limit State (SLS) in a chloride environment according to French standards.

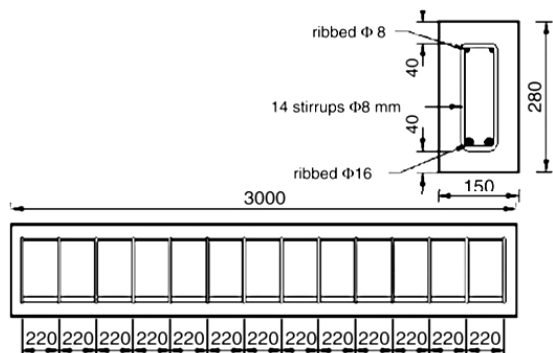


Fig. 1. Reinforcement Layout for Beams type A.

2.1 Material properties

2.1.1 Concrete properties

One vibrated concrete was used to cast the control beam. The average compression strength and the elastic modulus obtained on cylindrical specimens ($\varnothing 11 \times 22$ cm) were 45 MPa and 32 GPa respectively at 28 days. The tensile strength, measured using the splitting test, was 4.7 MPa. Porosity was 15.2%. To measure concrete characteristics, cylindrical cores, 70×140 mm, were drilled out of each beam and were tested in both compression and tension. Table 1, gives the results of those core tests.

Table 1. Mechanical characteristics of the concrete.

Mechanical characteristics	A1CL3	A1T
Compression strength (MPa)	62.15	58.90
Tensile strength (MPa)	6.85	5.98
Elastic modulus (MPa)	33 725	29 705

2.1.2 Characterization of steel bars, CFRP bars and filling material

The steel reinforcing bars were composed of natural S500 half-hard steels; ordinary ribbed reinforcing steel bars were used. The steel bars characteristics were measured after extracting the corroded steel bars out of the corroded beam A1CL3 and they were found as in Table. 2. Table 3 shows the mechanical properties of the

CFRP rods that found on that paper and the mechanical properties given by the manufacturer and by Laboratory test [11]. In order to increase the bond between the CFRP rods and the filling material, the CFRP rods were coated with 0.2/0.3 mm.

Table 2. Steel bars properties.

Specimen Type	elasticity modulus (GPa)	Yield Strength (MPa)	Ultimate Strength (MPa)
Corroded specimen	200	578	710
Non-corroded specimen	214	600	645

Table 3. CFRP rods characteristics.

Type of test	Ultimate strength (MPa)	Modulus of Elasticity (MPa)
Manufacturer's test	2300	150000
Laboratory test [11]	1875	145900

Table 4., shows the characteristics of the filling material (epoxy resin) after 7 days [10].

Table 4. Filling material properties.

Material	Compressive Strength (MPa)	Tensile Strength (MPa)	Elastic Modulus (MPa)
Epoxy	83	29.5	4900

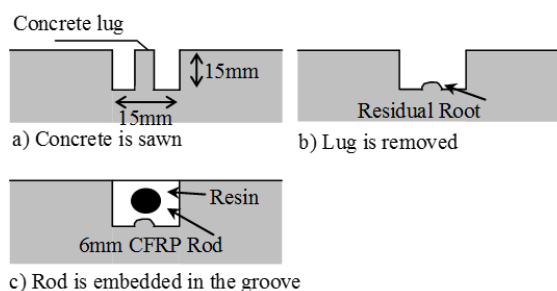


Fig. 2. Installation of CFRP rod into concrete surface.

2.2 Repair technique with NSM against flexural and shear forces

The NSM CFRP rod was installed in the corroded beam A1CL3 and in the control beam A1T by making two cuts in the concrete cover in the longitudinal direction at the tension side. A special concrete saw with a diamond blade was used. The groove was 15 mm deep (only 20 mm of concrete cover for beams) and 15 mm wide (around twice the rod diameter) [12]. The two beams were tested after 1 week of installing the CFRP rod in order to ensure the maximum degree of adhesion

between the concrete surface and the epoxy resin material. Figure 3 shows the final shape of the repaired beams after levelling the surface. After the two full span length for both beams A1CL3 and A1T were loaded up to failure, the four edges (A1CL3-SB, A1CL3-B, A1T-SB and A1T-B) in figure 4 were cut out of the full span for both beam A1CL3 and A1T.



a. A1T Control.Beam b. A1CL3 Corroded. Beam

Fig. 3. Concrete surface after installing the CFRP rod.

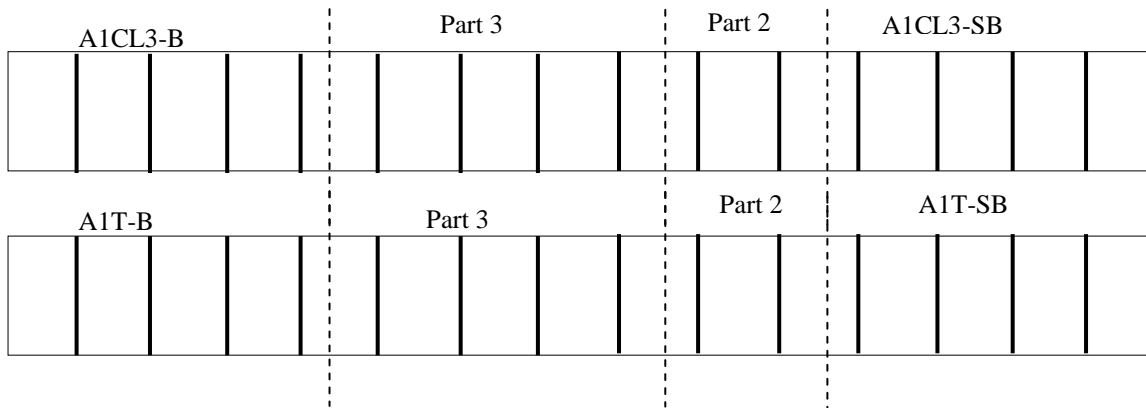


Fig. 4. Parts of corroded (A1CL3) and control beam (A1T).

The two edges (A1CL3-B and A1T-B) were re-repaired in bending only by removing the cracked areas of the epoxy resin material and install new material instead as shown in figure 5.



a. Before Re-repairing. b. After Re-Repairing.

Fig. 5. Re-repairing with NSM in bending.

Table 5. Parts of corroded and control beams.

Part number after repairing	Position	Length (cm)	Notes
A1CL3-SB	Right	80	Repaired in shear and bending
A1T-SB	Right	80	Repaired in shear and bending

Part 2	-	40	Damaged Area
Part 3	-	100	Damaged Area
A1CL3-B	Left	80	Repaired in bending
A1T-B	Left	80	Repaired in bending

The two edges (A1CL3-SB and A1T-SB) were re-repaired in bending and in shear using the configuration shown in figure 2. Four rods were installed on each side of each edge spaced with 10cm. The same procedure and technique followed for installing the rods shown in figure 4. Figures 6a, 6b present the two edges (A1T-SB and A1CL3-SB) after the repairing in shear.



Fig. 6.a A1T-SB after repairing in shear.



Fig. 6.b A1CL3-SB after repairing in shear.

2.3 Effect of corrosion on residual strength of steel bars

In order to remove the corrosion out of the steel bars surface a clark's solution ANSI/ASTM G1-72 was used to clean the surface of the bars, then the effect of corrosion on the diameter loss of the steel reinforcement bars was measured using mass loss method [10].

2.4 Beams Instrumentation

Ends slip during loading was measured using LVDT fixed at the end of each steel bar from both faces as shown in Figure 7.

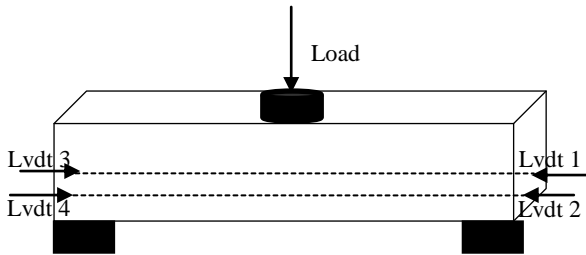


Fig. 7 Beams Instrumentation.

3 Experimental results

3.1 Corrosion results for steel bars and steel stirrups for corroded beams A1CL3-B and A1CL3-SB

The diameter loss percentage was measured along the two corroded beams A1CL3-B and A1CL3-SB, the maximum diameter loss was found 18 % at 28 cm away of the mid-span of A1CL3-B while 9 % diameter loss was found in A1CL3-SB at 20 cm away of the mid span. Figure 8 presents the diameter loss percentage for tensile steel bars at every location along the two corroded beams. The maximum diameter loss found in beam A1CL3-B was 86% at stirrup 4-4 while the maximum loss in A1CL3-SB was 61% at stirrup 1-1, figures 8 and 10.

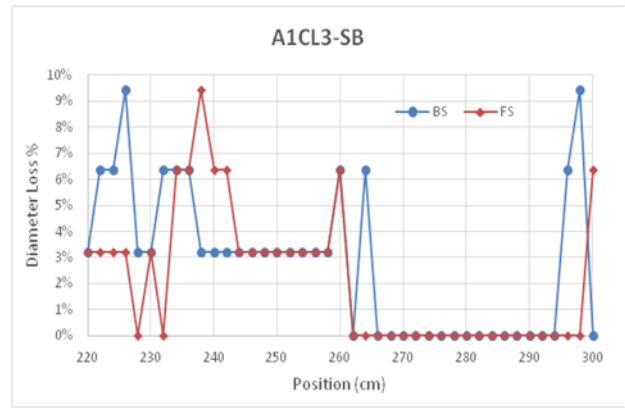
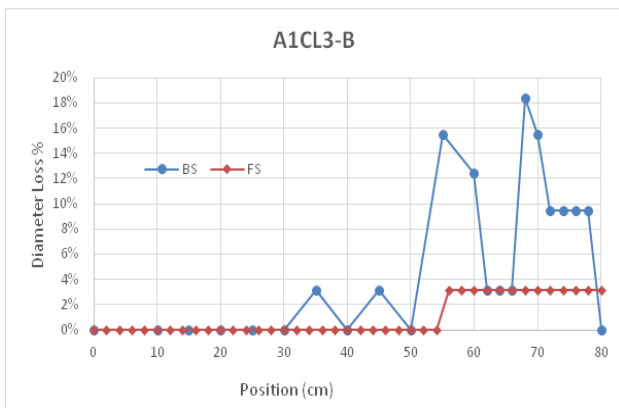


Fig. 8 Diameter loss percentage in corroded beams. The steel stirrups were numbered regarding to their parts as shown in figure 9

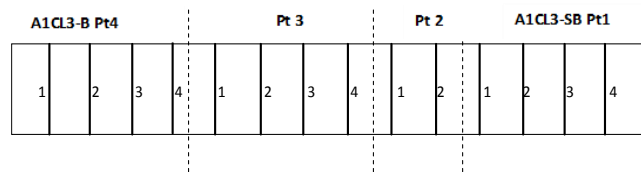


Fig. 9 Stirrups numbering of beams A1CL3.

Figure 10, shows the locations of corrosion in steel stirrups and the diameter values. No corrosion was found in stirrups 4-1 and 4-2

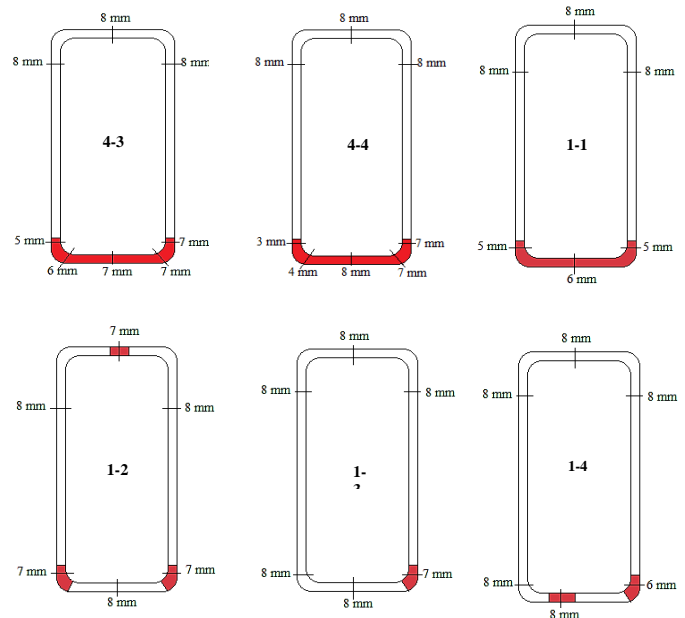


Fig. 10 Locations of corrosion in steel stirrups.

3.2 Ultimate load capacity and failure modes

Figure 11 shows the ultimate load capacity of the four beams versus the deflection values.

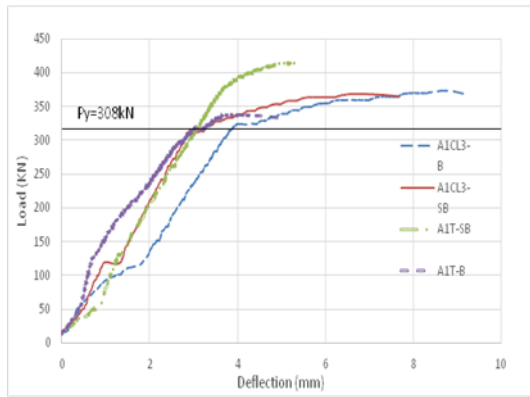
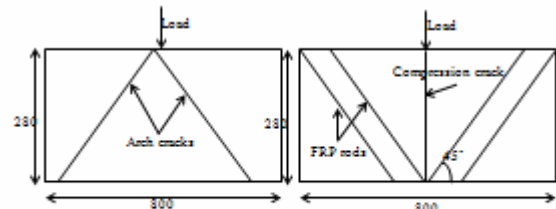


Fig. 11 Load capacity vs deflection for beams.

Non shear repaired beams A1T-B and A1CL3-B failed by diagonal tension failure. The shear repaired control and corroded beams A1T-SB and A1CL3-SB respectively failed by crushing of compressed concrete (figures 12, 13). The shear repaired control beam A1T-SB failed at 414.6 kN which was higher than the ultimate load capacity of non shear repaired control beam A1T-B which failed at 337.4 kN. The ultimate load capacities of shear repaired corroded beam A1CL3-SB and the non-repaired one A1CL3-B were close to each other (367.8 kN and 373.3 kN respectively) and higher than the ultimate load for of non shear repaired control beam A1T-B (337.4 kN). Figure 11 shows that the shear repaired beams A1T-SB and A1CL3-SB showed a higher rigidity than the non shear repaired beams A1T-B and A1CL3-B.



Fig. 12 Failure modes for four beams.



a. With shear strengthening b. Without shear strengthening.

Fig. 13 Two kinds of failure modes.

3.3Slip measurement

Figure 14 shows the slip measurements for tensile steel bars of the four tested beams.

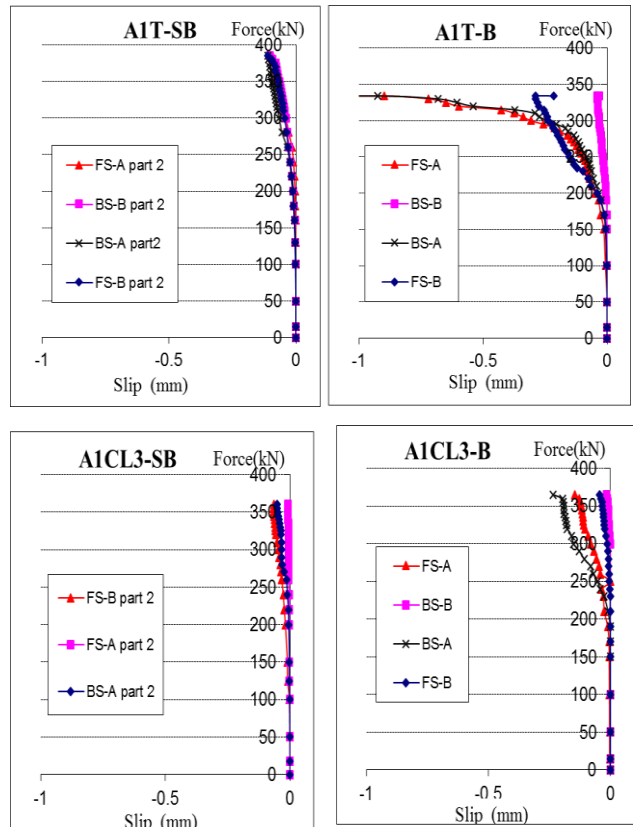


Fig. 14 Slip measurements for four tested beams.

The slipping of the steel bars in repaired corroded beam in bending only (A1CL3-B) started at 250 kN and 200 kN for the control beam (A1T-B). Beams tested by [13] showed that slipping started at 100 kN and 150 kN. The maximum slip value found in control beam A1T-B was larger than the slip value in corroded beam A1CL3-B (1mm and 0.23 mm respectively) which agrees with [14] that showed an enhancement in the anchorage capacity between steel and concrete in the corroded beams due to the increased radial stresses on the bar-concrete interface of the end points of beams. If the repaired beams in shear A1T-SB and A1CL3-SB are compared to non-repaired beams, it is very clear that repairing in shear with NSM decreased significantly the maximum slip values (from 0.23mm to 0.05mm for A1CL3 and from 0.92 to 0.09).

3.3.1 Effect of corrosion

The first arch crack happened in beam A1CL3-B was at 10 cm of the support where at this point there was no corrosion as shown in figure 8 so there is no relationship between the corrosion percentage and the arch failure effect.

3.3.2 Effect of NSM FRP rods in increasing the shear capacity

Table 6 presents a comparison between all beams (corroded and control) in terms of steel loss and load capacity. Table 6 shows that the repaired beam in shear and bending in this paper (A1CL3-SB) gave an increase percentage of 30% and 38% in the ultimate load capacity than in the non-repaired corroded beams (A2CL3-B, A2CL3-A respectively) tested by [13].

Table 6. Comparison between all beams.

Beam	Max. loss in bars %	Max. loss in stirrups %	Load capacity (kN)	Load capacity increase compared to A1CL3-SB %
A1T-B	0	0%	337	-
A1T-SB	0	0%	415	-
A1CL3-B	18	86%	373	-
A1CL3-SB	9	61%	368	-
A2T[9]	0	0%	261	29
A2CL3-A[9]	25	36%	230	38
A2CL3-B [9]	21	60%	256	30

3.3.3 Arch phenomena

In order to calculate the yielding force capacity P, the following conventional equilibrium equation was used:

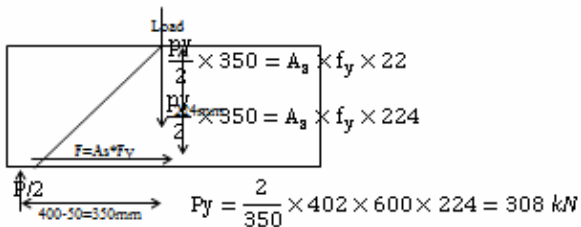


Fig. 15 Calculation of Py

The calculated yielding force Py agrees with the experimental results for non-repaired beams in shear A1T-B and A1CL3-B as shown in figure 11.

4 Conclusions

The following conclusions can be drawn: The failure of all repaired RC beams (corroded and control) in flexion only was by shear failure after CFRP rods slip, the failure

of all RC beams (corroded and control) repaired in both flexion and shear occurred due to concrete crushing While the Repairing against shear using NSM FRP rods increases the ultimate shear capacity of beams (30% and 38%) for corroded and control beams respectively. The corrosion didn't affect the ultimate shear capacity of beams. Repairing against shear using NSM FRP rods decreases significantly the maximum slip of the steel bars.

References

1. A. Almusallam Effect of degree of corrosion on the properties of reinforcing steel bars. Constr Build Mater **15**:361–368. (2001)
2. C. Andrade, C. Alonso, D. Garcia, J. Rodriguez Remaining lifetimes of reinforced concrete structures: effect of corrosion on the mechanical properties of the steel. NACE, Cambridge, UK, pp 546–557. (1991)
3. A. Rizzo, L. De Lorenzis, Modeling of debonding failure for RC beams strengthened in shear with NSM FRP reinforcement, Proceedings FRPRCS8, Patras, Greece, Luglio. (2007)
4. M. Jalili, M. Sharbatdar, J. Chen, F. Alaei. Shear strengthening of RC beams using innovative manually made NSM FRP bars, Construction and Building Materials **36**: 990-1000. (2012)
5. L. De Lorenzis, A. Nanni, A. La Tegola. Flexural and Shear Strengthening of Reinforced Concrete Structures with Near Surface Mounted FRP Rods. In 521-528. Ottawa, Canada. (2000)
6. A. Nanni, M. Ludovico, R. Paretto, Shear Strengthening of a PC Bridge Girder with NSM CFRP Rectangular Bars, Advances in Structural Engineering Vol. **7** No. 4 2004: p.97-109. (2003)
7. L. De Lorenzis, A. Nanni. Shear strengthening of reinforced concrete beams with near surface mounted fibre reinforced polymer rods. ACI Structural Journal **98**(1): p.60-68.(2001)
8. A. Castel, R. François, G. Arliguie, Mechanical behaviour of corroded reinforced concrete beams Part1: Experimental study of corroded beams. RILEM Materials and Structures **33**: 539–544.(2000)
9. T. Vidal, A. Castel, R. François. Corrosion process and structural performance of a 17 year old reinforced concrete beam stored in chloride environment. Cement and Concrete Research **37**(11): p.1551-1561.(2007)
10. A. Kreit, F. Al-Mahmoud, A. Castel, R. François, Repairing corroded RC beam with near-surface mounted CFRP rods. Materials and Structures **43**(9). (2010)
11. F. Al-Mahmoud, A. Castel, R. François, C. Tourneur, Effect of surface preconditioning on bond of carbon fibre reinforced polymer rods to concrete. Cement & Concrete Composites **29**(9): p.677-689. (2007)
12. F. Al-Mahmoud, A. Castel, R. François, C. Tourneur, Anchorage and tension stiffening effect between near-surface mounted fibre-reinforced

polymer rods and concrete. 2nd International RILEM Symposium on Advances in Concrete through Science and Engineering.(2006)

13. I. Khan, Etude expérimentale de la corrosion en béton armé Ph.D Thesis. UNIVERSITÉ DE TOULOUSE, France. (2012)
14. J. Cairns, Y. Du, D. Law, Structural performance of corrosion-damaged concrete beam, Magazine of Concrete Research, vol. **60**, no. 5, pp. 359-370. (2008)